The Rafita asteroid family

Safwan Aljbaae, V Carruba, J R Masiero, R C Domingos, M Huaman

The Rafita asteroid family

S. Aljbaae,[1]⋆ V. Carruba,[1]⋆ J. R. Masiero,[2] R. C. Domingos[3] and M. Huaman[1]

[1]*Faculdade de Engenharia, Universidade Estadual Paulista (UNESP), Guaratinguetá , CEP 12516-410, SP, Brazil*
[2]*Jet Propulsion Laboratory/Caltech, 4800 Oak Grove Dr., MS 183-601, Pasadena, CA 91109, USA*
[3]*Universidade Estadual Paulista (UNESP), São João da Boa Vista, CEP 13874-149, SP, Brazil*

ABSTRACT

The Rafita asteroid family is an S-type group located in the middle main belt, on the right-hand side of the 3J:-1A mean-motion resonance. The proximity of this resonance to the family left-hand side in the semimajor axis caused many former family members to be lost. As a consequence, the family shape in the (a, $1/D$) domain is quite asymmetrical, with a preponderance of objects on the right-hand side of the distribution. The Rafita family is also characterized by a leptokurtic distribution in inclination, which allows the use of methods of family age estimation recently introduced for other leptokurtic families such as Astrid, Hansa, Gallia and Barcelona. In this work, we propose a new method based on the behaviour of an asymmetry coefficient function of the distribution in the (a, $1/D$) plane to date incomplete asteroid families such as Rafita. By monitoring the time behaviour of this coefficient for asteroids simulating the initial conditions at the time of the family formation, we were able to estimate that the Rafita family should have an age of 490 ± 200 Myr, in good agreement with results from independent methods such as Monte Carlo simulations of Yarkovsky and YORP dynamical induced evolution and the time behaviour of the kurtosis of the $\sin(i)$ distribution. Asteroids from the Rafita family can reach orbits similar to 8 per cent of the currently known near-Earth objects. During the final 10 Myr of the simulation, $\simeq$1 per cent of the simulated objects are present in NEO space, and thus would be comparable to objects in the present-day NEO population.

Key words: celestial mechanics – minor planets, asteroids: general.

1 INTRODUCTION

Asteroid families are groups of minor planets originated by catastrophic disruption events of single parent bodies, identified by clustering in their proper orbital elements, which are very close to invariants of motion characterizing their orbits. A typical asteroid family shows a clear V-shape in the distribution of associated asteroids in the (proper a, H) or (proper a, $1/D$) plane, where a, H and D are the asteroid proper semimajor axis, absolute magnitude and diameter, respectively. Morbidelli, Thomas & Moons (1995) showed that families located near the boundary of resonant zones in the main asteroid belt might have importantly contributed to the near-Earth material and, consequently, also to the cratering history of the Earth or Moon. For instance, asteroids near the 3J:-1A resonance with eccentricities less than 0.1 would undergo small variations in eccentricity on time-scales of million years, and then suddenly they undergo eccentricity increases to over 0.3, becoming Mars-crossers, and a possible source for Earth-crossing materials (Wisdom 1983).

Among main belt families, the Rafita family is an S-complex group. In total, 1295 members of this family were identified in Nesvorny, Broz & Carruba (2015) using the hierarchical clustering method (HCM), described in Bendjoya & Zappalà (2002), with a distance cut-off of 70 m s^{-1}. The Rafita family is located in the central main belt between the 3J:-1A and 11J:-4A mean-motion resonances. Its values of the a, e and $\sin(i)$ proper orbital elements go from 2.53 to 2.65 au, 0.15 to 0.20 and 0.11 to 0.15, respectively. The global structure of this family seems to have been significantly affected by the 3J:-1A resonance. The family is characterized by only one side of its V shape, with its left-hand side presumably missing because of the interaction of former family members with this resonance (Spoto, Milani, & Knežević 2015).

Based on this last hypothesis, we aim in this work to investigate in detail the local dynamical evolution of asteroids in the Rafita family, analysing the past leakage of the family members to the 3J:-1A resonance, and to check what information the family age and dynamical evolution of the peculiar orbital configuration of this group it may provide. In particular, by quantifying the current level of asymmetry in semimajor axis and $1/D$ of the family through the use of a C-target function and a newly introduced asymmetry

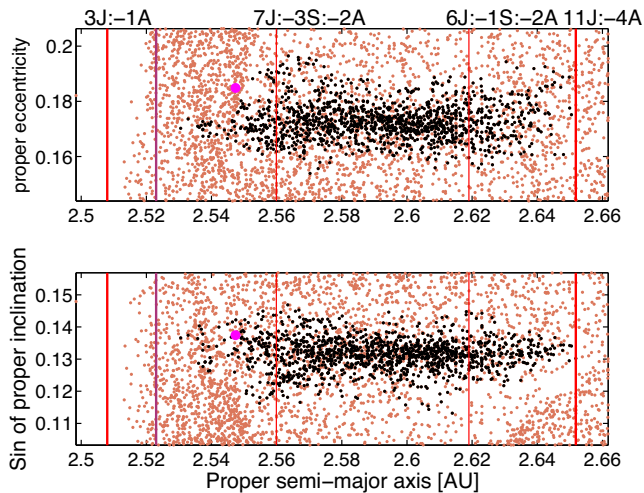⋆ E-mail: safwan.aljbaae@gmail.com (SA); vcarruba@gmail.com (VC)

Figure 1. A projection in the (*a*, *e*) (top panel) and [*a*, sin (*i*)] (bottom panel) domains of members of the HCM Rafita cluster (1295 members, black dots) and of the local background (3987 members, orange dots). Vertical red lines display the local mean-motion resonances.

coefficient A_S, and by studying the time behaviour of this parameter for fictitious Rafita family members simulating the initial conditions of the family at the time of the breakup, we propose to introduce a new method to obtain age estimates for asteroid groups interacting with powerful mean-motion resonances. Preliminary estimates of the contribution to the near-Earth asteroid (NEA) population from the Rafita family will also be attempted in this work.

2 FAMILY IDENTIFICATION AND PHYSICAL PROPERTIES

A set of 406 253 proper elements of numbered asteroids from the AstDyS[1] in the (*a*, *e*) and [*a*, sin (*i*)] planes, and the orbital locations of the family members are shown as full black dots in Fig. 1, where local background asteroids are also drawn as full orange dots. The HCM family represents about 32 per cent of the asteroids in its region. Vertical heavy and light red lines display the location of the main two- and three-body mean-motion resonances in the region, respectively. The indigo line displays the chaotic layer near the 3J:-1A resonance, as defined in Morbidelli & Vokrouhlický (2003). That corresponds to a zone within 0.015 au from the resonance boundary, where the asteroid population is depleted because of the presence of several high-order mean-motion resonances. The position of 1644 Rafita itself is shown as a magenta full dot.

We then revised the physical and taxonomic properties of the objects in the Rafita region. Only nine objects had taxonomic data (4 S-,2 X-, 1 Ch- and 1 Sa-types), observed during the second phase of the Small Mainbelt Asteroid Spectroscopic Survey (SMASS II[2]), which used the feature-based taxonomy of Bus (1999) and Bus & Binzel (2002a,b). Also, using the photometric data from the Fourth Release of the Sloan Digital Sky Survey Moving Object Catalog
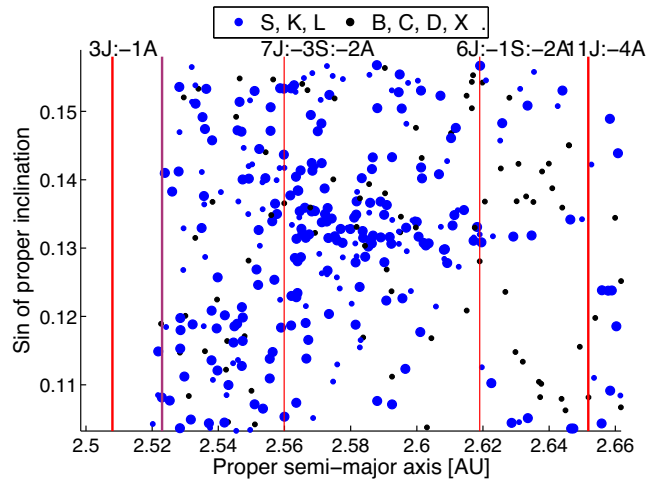

Figure 2. An [*a*, sin (*i*)] projection of the 374 asteroids in the Rafita region with taxonomic information from the SDSS-MOC4 data base. See the figure legend for the meaning of the full dot symbols; other symbols are the same as in Fig. 1.

(SDSS-MOC4[3]; Ivezić et al. 2001), taxonomic information for 374 asteroids was obtained with the method described in DeMeo & Carry (2013), computing the spectral slopes over the *g′*, *r′* and *i′* reflectance and the *z′* − *i′* colours. We found 191 S-, 55 L-, 45 K-, 38 C-, 34 X-, 8 D-, 2 B- and 1 V-types. Only one asteroid had taxonomic data in the SMASS II classification in the Rafita HCM group: 1587 Kahrstedt (SA). A total of 123 asteroids in the HCM group had taxonomic information in the SDSS-MOC4 data set: 72 S-, 21 K-, 17 L-, 8 X-, 3 C-, 1 D- and 1 V-types. The 12 X-, C-, D- and V-type objects, corresponding to 9.8 per cent of the objects with taxonomic information, can be considered as taxonomic interlopers of the S-complex Rafita family, and will be excluded from the family list. As shown in Fig. 2, the S-complex objects dominate the local background, but with a significant mixing with other-type objects.

Regarding the albedo information, the *Wide-field Infrared Survey Explorer* (*WISE*) and Near-Earth Object WISE [4] data (Masiero et al. 2011) were used to identify 449 bodies of the local background with geometric albedos p_V varying between 0.022 and 0.531. Of these 449 objects, a total of 339 objects do not have taxonomic information. About half of those last albedos values vary between 0.12 and 0.30, and this suggests that they may be compatible with an S-complex composition. About 28 per cent have an albedo greater than 0.3. The remaining 22 per cent have low albedos (lower than 0.12), which is usually associated with a C-complex taxonomy (Masiero et al. 2011). The [*a*, sin (*i*)] projection of the 449 objects with albedos in the region is displayed in Fig. 3. In the Rafita HCM group, there are 154 asteroids with identified albedos between 0.036 and 0.53. The mean albedo found in the group is 0.243, and the median one is 0.247.

An estimate for 154 effective diameters (*D*) of asteroids in the Rafita HCM group is also provided in the *WISE* data. The diameters of the remaining objects were computed according to equation (1) in Carruba et al. (2003). The obtained diameters vary between 0.644 (323442 2004 HB1) and 17.472 km (6076 Plavec). Therefore, the Rafita family is formed mostly by small-diameter objects, and could be the result of a catastrophic disruption event.
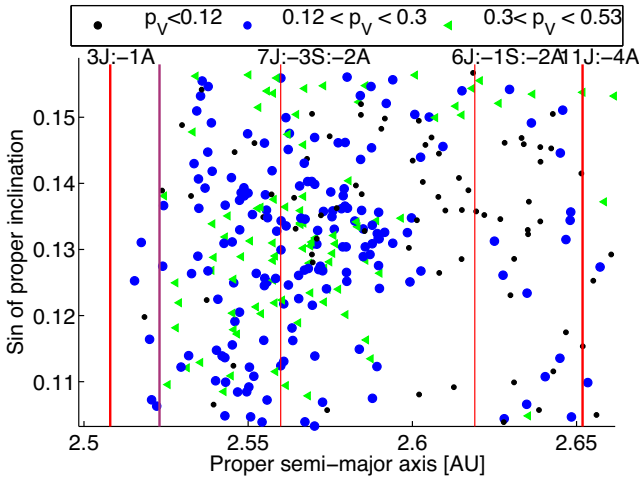

Figure 3. An [a, $\sin(i)$] projection of the 449 bodies in the Rafita region with albedos information from the *WISE* data set. See the figure legend for the meaning of the full dot symbols; other symbols are the same as in Fig. 1.

The total mass of the family is estimated as 0.618×10^{17} kg, assuming a spherical shape, a homogeneous structure for each asteroid with densities according to the values typical for each class (DeMeo & Carry 2013). For objects without taxonomical information, a mean density value of 2.91 g cm^{-3} was assumed. This density is within the typical densities of S-type asteroids (2.72 ± 0.54; DeMeo & Carry 2013). Overall, the total mass of the family as estimated in this work suggested that the Rafita family originated from the breakup of a $D \simeq 45$ km asteroid in the region, i.e. a medium-sized asteroid.

3 DYNAMICAL MAP

Many features of the asteroid distribution observed in Fig. 1 may be explained by the long-lasting effects of dynamical evolution. Constructing dynamical maps for the region of Rafita can be useful to improve our understanding of the local dynamics. For this task, the SWIFT_MVFS symplectic integrator from the SWIFT package (Levison & Duncan 1994), modified by Brož (1999), was used to integrate 6205 massless particles over 20 Myr. The initial conditions varied between 2.49 and 2.66 au in a, and between 1°.00 and 9°.6 in i. An equally spaced grid in the [a, $\sin(i)$] plane was generated using 85 intervals in a and 73 in i. The initial values of the eccentricity e, longitude of the ascending node Ω, argument of pericentre ω and true anomaly λ were fixed at those of the asteroid (1644) Rafita at J2000. Synthetic proper elements and frequencies were computed with the approach described in Carruba (2010).

Fig. 4 shows the dynamical map in the proper [a, $\sin(i)$] plane for 6205 particles in the orbital neighbourhood of Rafita. Black full dots identify the values of proper elements. Vertical alignments in the map are associated with mean-motion resonances. Due to their dynamical importance, we choose to display as light red lines the orbital location of only two resonances (the 7J:-3S:-2A and 6J:-1S:-2A) listed in Nesvorný & Morbidelli (1998). The proper elements of real objects in the Rafita HCM dynamical group, obtained after integrating these bodies with the same scheme as used to obtain the dynamical map, are also plotted over the dynamical map as blue full dots. Many resonances cut through the group, and, as a consequence, several family members are expected to be in these resonances. A detailed analysis of the local dynamics was performed in Carruba et al. (2007); interested readers could find
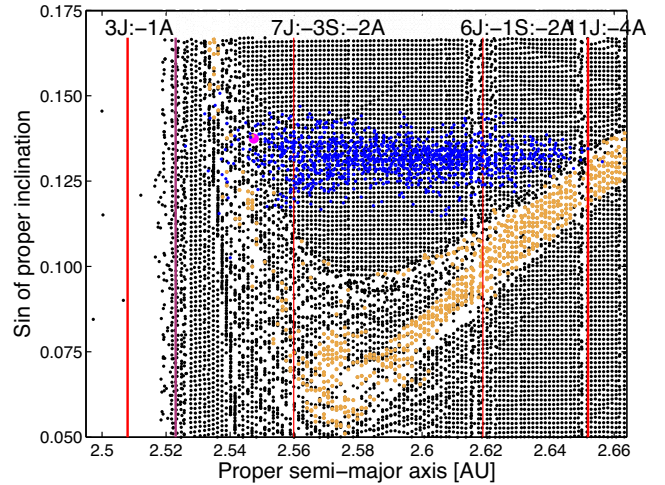

Figure 4. An [a, $\sin(i)$] proper element map of the Rafita region. Proper elements of test particles are shown as black full dots. The $g + g_5 - 2g_6$ secular resonance is marked by amber full points. Other symbols are the same as in Fig. 1.

more details about this region in that paper. Here we just emphasize the role of the $g + g_5 - 2g_6$ secular resonance, which is the resonance affecting the largest number of asteroids in the region. Objects whose pericentre frequency is within ± 0.3 arcsec yr^{-1} from $g = 2g_6 - g_5 = 52.229$ arcsec yr^{-1}, i.e. objects that are more likely to be in librating states of a four-order non-linear secular resonance (Carruba 2009), are marked in amber.

4 AGE OF THE RAFITA FAMILY

In this section, the method of Yarkovsky isolines is first used to preliminary assess the possible age of the family and to attempt eliminating possible dynamical interlopers, i.e. objects whose current orbit could not be explained as having diffused to its current location to within the maximum estimate of the family age (Carruba, Aljbaae & Souami 2014; Carruba et al. 2015). For this purpose, the isolines of equal displacement induced by the Yarkovsky force were computed for different estimated ages at the position of the family centre. In fact, one problem with this method is what is considered for the family centre. In this work, we computed isolines of maximum displacement in a for a fictitious family originating at the current location of 1644 Rafita itself. We used the parameters affecting the Yarkovsky force for S-type asteroids, as listed in Brož et al. (2013): $\rho_{\mathrm{surf}} = 1500$ and $\rho_{\mathrm{bulk}} = 2000$ kg m^{-3} for the surface and bulk densities, $C = 680$ J kg^{-1} K^{-1} for the thermal capacity, $A = 0.1$ for the Bond albedo, $\epsilon_{\mathrm{IR}} = 0.9$ for the thermal emissivity and $K = 0.01$ W m^{-1} K^{-1} for the surface thermal conductivity. (With respect to Brož et al. (2013), we are using a larger value of K and a lower value of ρ_{bulk} because most of the Rafita members are few-km-sized asteroids, characterized by higher values of K and lower densities; see Delbo et a. 2015.) The uncertainty by which these parameters are known is, however, one of the main sources of error for asteroid family dating (Masiero et al. 2012). We warn the reader that other possible choices of K and ρ_{bulk} could produce different values of the family age.

Fig. 5 displays the location of the Rafita family members in the (a, D) domain. Rafita itself, with a *WISE*-estimated diameter of 15.57 km, is shown as a magenta full dot. The concentration of large objects towards the border of the 3:1 mean-motion resonance
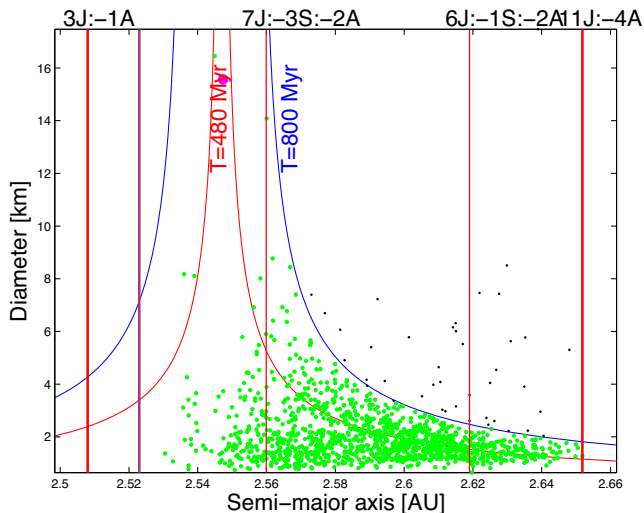
Figure 5. A proper *a* versus radius projection of members of the Rafita family. The red and blue lines display the lines of equal Yarkovsky displacement for $T = 480$ and 800 Myr, respectively.

indicates that the original structure was affected by this resonance. One problem with the application of the method of isolines of equal displacement caused by the Yarkovsky effect is what is considered for the family centre. For families formed in non-catastrophic events, the centre can be assumed to coincide with the largest remnant. Alternatively, the use of the centre of mass can be used for the cases of families formed by catastrophic disruption events.

Rafita, however, is peculiar because (i) it was formed in a catastrophic event, (ii) most of the objects on the left-hand side of the family were lost in the 3J:-1A mean-motion resonance, and (iii) (1644) Rafita itself could have migrated by up to 0.005 au outwards or inwards over the estimated $\simeq 0.5$ Gyr age of the family, assuming a maximum Yarkovsky drift rate for an asteroid of this size, and $0°$ or $180°$ stable spin obliquity. Since the current barycentre of the Rafita family is not a viable option because of the family incompleteness, we computed isolines of maximum displacement in *a* for a fictitious family originating at the current location of 1644 Rafita itself (Fig. 5). Errors possibly caused by the Yarkovsky induced uncertainty in the position of 1644 Rafita will be accounted for later on in this paper.

Isolines were computed for times equal to 480 Myr, the estimated age according to Nesvorny et al. (2015) and Carruba & Nesvorný (2016) using a V-shape criterion, and 800 Myr, respectively, which is quite larger than the maximum estimate of the family age (580 Myr) found in the literature. Since this method does not account for the initial dispersion of the family members, ages obtained with this method can be overestimated. The 43 asteroids outside the maximum Yarkovsky isoline in Fig. 5 were considered dynamical interlopers and excluded from the family list.

Yarkovsky isolines do not provide an optimal estimate of asteroid families' ages, since they neglect the effect of the initial ejection velocity field. However, they can be used to obtain a preliminary value that can be later refined by a more advanced method. In this work, we also used the Yarko–YORP Monte Carlo method of Vokrouhlický et al. (2006a,b,c) to obtain a more precise estimation of the age and ejection velocity parameter. We modelled the evolution of simulated family members due to Yarkovsky and YORP forces over time intervals of the order of the age of the family. This method was modified by Carruba et al. (2015) to include the stochastic version

of the YORP effect (Bottke et al. 2015). Modelling the diffusion via YORP effects, a target function *C* for each body is defined as

$$0.2H = \log_{10}\left(\frac{\Delta a}{C}\right), \tag{1}$$

where *H* is the absolute magnitude of the body and $\Delta a = a - a_b$, where a_b is the family centre, assumed equal to the current position of 1644 Rafita. The distribution of the family members can be characterized using a one-dimensional array $N_{obs}(C)$ indicating the number of asteroids in the interval $(C, C + \Delta C)$. The histogram of the target function *C* for the Rafita family is presented as a blue line in Fig. 6, panel A. A total of 33 intervals are used starting at $C_{min} = -6.6 \times 10^{-5}$ with a step of 4.0×10^{-6} au. Errors are assumed to be proportional to the square root of the number of asteroids in each *C* bin. To account for the uncertainty in the original orbital position of Rafita, we computed an average of five *C* distributions, one centred at the current orbital position of Rafita and two each at ± 0.5 and ± 1 of the maximum drift in *a* caused by the Yarkovsky effect (0.005 au). Because the Rafita family is currently incomplete at lower values of semimajor axis (and therefore of *C*), we neglected negative *C* values in our analysis (shown as grey in Fig. 6). Since we are using only the positive *C* distribution to estimate two parameters, our distribution has 15 (17 − 2) degrees of freedom.

Following the work of Carruba et al. (2014, 2015, 2016), fictitious distributions of asteroids were evolved for different values of the ejection velocity parameter V_{EJ} [see for instance, equation (3) in Carruba et al. (2016) for a definition of this parameter], considering the Yarkovsky effect (both diurnal and seasonal versions), and the stochastic YORP torque. Assuming that about half of the family was lost in the 3J:-1A mean-motion resonance, and considering a density of S-type bodies, a parent body of 45 km in diameter was considered to estimate an escape velocity as $V_{esc} = 28$ m s^{-1}. During the investigation of the shape of the ejection velocity field of 49 asteroid families by Carruba & Nesvorný (2016), it was found that the typically observed values of $\beta = \frac{V_{EJ}}{V_{esc}}$ did not generally exceed 1.5. Thus, the maximum values of V_{EJ} considered here will be 50 m s^{-1}. Results for $V_{EJ} > 50$ m s^{-1} will not be shown, for simplicity. The distributions of the *C* function for the simulated family are then compared with that for the real one (supposing a half of it was lost by the 3J:-1A mean-motion resonance), minimizing a χ^2-like function $\psi \Delta C$ [see equation (6) in Carruba et al. 2016].

The values of $\psi \Delta C$ in the (Age, V) plane are presented in Fig. 6, panel B. For 15 degrees of freedom, and assuming that the $\psi \Delta C$ follows an incomplete gamma function distribution (Press et al. 2001), the value $\psi \Delta C = 13.53$ (red line in Fig. 6, panel B) is associated with a 1σ probability of 68.3 per cent that the simulated family and the real one are compatible. Our results are compatible with the estimate from Nesvorny et al. (2015): We find an age of 490^{+190}_{-220} Myr, and a value of the ejection velocity parameter of 20^{+50}_{-20} m s^{-1}, compatible with the estimated escape velocity from the parent body ($\beta = 0.71$). In the next section, we will analyse the dynamical evolution of fictitious families obtained with this value of V_{EJ}, and discuss what constraints on the family age can be obtained by these numerical experiments.

5 DYNAMICAL EVOLUTION OF THE RAFITA FAMILY

Numerical integration with the SWIFT_RMVSY code from the SWIFT package (Levison & Duncan 1994), which uses the Regularized Mixed Variable Symplectic method, modified by Brož (1999), was performed over 800 Myr in order to investigate the dynamical
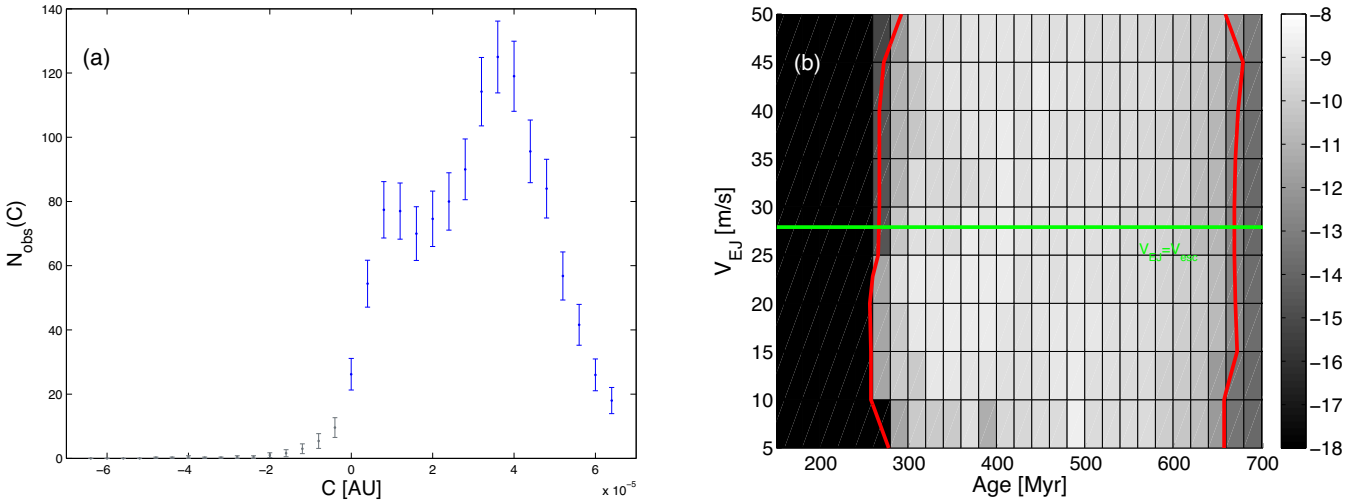
Figure 6. Panel A: a histogram of values of the C target function from equation (1) for the Rafita family. Panel B: values of the $\psi \Delta C$ function in the (Age, V) plane, for simulated Rafita families.

evolution of Rafita fictitious family members, obtained with the approach described in the previous section and $V_{EJ} = 20$ m s^{-1}. The SWIFT_RMVSY integrator allows to integrate a set of massless test particles (which do not interact among themselves) under the gravitational influence of all planets, considering the diurnal and seasonal versions of the Yarkovsky effect. Using the method outlined in Machuca & Carruba (2012), two spin-axis obliquities forming angles of 0° and 180° with the orbital angular momentum were used to investigate the maximum orbital mobility caused by the Yarkovsky effect. Synthetic proper elements for each test particle were obtained with the approach described in Carruba (2010).

Defining a Rafita orbital region with the method described in Section 2, we first checked the number of particles that remained in the region as a function of time. Results are shown in Fig. 7, panel A, where we display the percentile of surviving particles in the Rafita region as a function of time. The vertical red dashed line is associated with the estimated family age of 490 Myr, while the other vertical dashed lines are associated with the minimum and maximum estimated family ages, according to this work. At the estimated family age, only 36.9 per cent of the original family members remained in the Rafita region, which indicates that more than half of the family was lost because of a dynamical mechanism, mainly an interaction with the 3J:-1A mean-motion resonance. Since Carruba (2016) recently introduced a method based on the time behaviour of the kurtosis of the v_W component of the ejection velocity field [$\gamma_2(v_W)$] of families characterized by a leptokurtic distribution of this parameter, and since the Rafita family is one of the most leptokurtic families in the main belt [$\gamma_2(v_W) = 0.72$, Carruba & Nesvorný 2016, we also checked the time behaviour of this parameter for the simulated family. Results are shown in Fig. 7, panel B. Errors for the $\gamma_2(v_W)$ were computed assuming that they were equal to $\frac{\sqrt{24\sigma(v_W)^2}}{n}$, where $\sigma(v_W)$ is the standard deviation in v_W and n is the number of Rafita members (Kendall & Stuart 1969). Except for isolated spikes, associated with single particles that experienced sudden changes of inclination, the current value of $\gamma_2(v_W)$ was reached in time-scales compatible with those associated with the family estimated age.[5]

Motivated by this preliminary analysis, we continued our analysis by analysing the degree of asymmetry of the current Rafita family. As observed in Fig. 6, panel A, the current distribution of C values for the Rafita family is considerably asymmetric, with much fewer asteroids in negative C value bins than in positive ones. To quantify the degree of asymmetry of the Rafita family, we introduce an asymmetry coefficient A_S defined as

$$A_S = \frac{1}{N_{\text{ast}} \cdot N_{\text{int}}} \sum_1^{N_{\text{int}}} (N_{\text{pos}}(i) - N_{\text{neg}}(i)), \qquad (2)$$

where N_{ast} is the number of objects in the simulated Rafita family, $N_{\text{int}} = 17$ is the number of positive intervals in the C distribution, and $N_{\text{pos}}(i)$ and $N_{\text{neg}}(i)$ are the number of asteroids in the positive and negative ith bins of the distribution. A family with a larger population in positive C bins would have a positive A_S value, while the opposite would be true for families with larger populations in negative C bins. The current values of A_S for the Rafita family, when its centre is assumed to be at the current orbital location of (1644) Rafita, is 0.026 ± 0.003. We computed values of A_S for our simulated family using the current orbital location of (1644) Rafita, as a reference, as a function of time. Our results are shown in Fig. 8. Remarkably, we find a very good agreement with the age estimated from the analysis of A_S and that obtained from the other two previously described methods. In the next section, we will estimate the contribution to the NEA population from the Rafita family.

6 THE CONTRIBUTION TO THE NEA POPULATION FROM THE RAFITA FAMILY

Following the techniques described in Masiero et al. (2015a), we have performed numerical simulations of the evolution of small family members from the Rafita breakup event into near-Earth space.

---

[5] Results for these simulations were obtained under the assumption that the asteroid spin obliquity remains fixed at 0° or 180° during the simulation.

Including YORP random walking may affect the dispersion in inclination, and therefore affect the observed values of $\gamma_2(v_W)$. While we do not expect this effect to dramatically alter the time evolution of the $\gamma_2(v_W)$ on short time-scales, this may be important (or not) at longer time-scales. Assessing the importance of this effect for more evolved asteroid families remains, in our opinion, a challenge for future work.
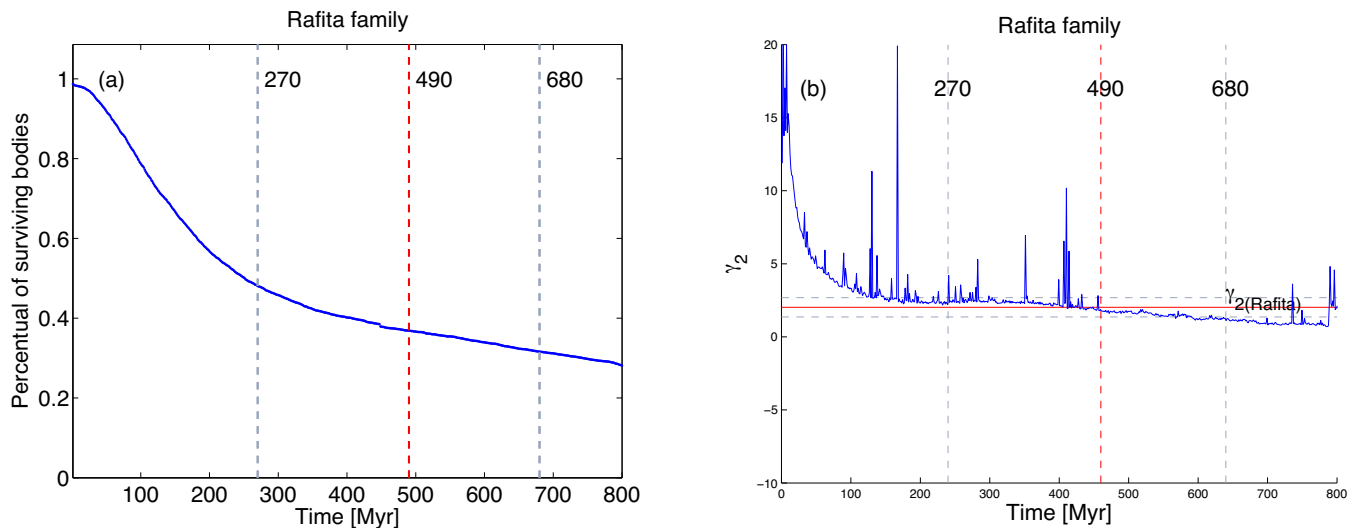
Figure 7. Panel A: percentile of surviving particles in the Rafita region as a function of time. Vertical dashed lines display the estimated age of the family, according to this work. Panel B: time behaviour of the kurtosis of the v_W component of the ejection velocity field $[\gamma_2(v_W)]$ for the simulated Rafita family. The horizontal red line displays the current value of the $\gamma_2(v_W)$ parameter for the Rafita group, while the horizontal dashed lines show the current value plus or minus its error.
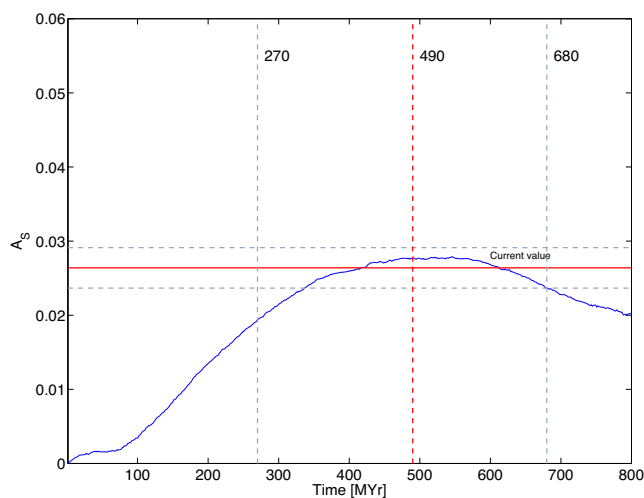

Figure 8. Asymmetry coefficient of the target function C, for the case where the centre of the family was assumed to be at the current location of (1644) Rafita. The horizontal lines display the current value of A_S for the Rafita family. Dashed horizontal lines display the current value of A_S plus or minus its error, obtained with standard error propagation formulas. Vertical lines have the same meaning as in Fig. 7.

Family members were randomly generated with initial ejection velocities matching our best-fitting velocity of 20 m s^{-1} around the current orbit of the presumed parent body (1644) Rafita. Particles were given the physical properties in the previous sections, a geometric albedo following the family mean of $p_V = 0.26$ and a diameter randomly drawn from the current family size frequency distribution (Masiero et al. 2015b), between 1 and 7 km.

Family members were forward-integrated for 500 million years using SWIFT_RMVSY. Spin axes were initially randomized, and evolved under YORP and collisional reorientation. When a family member entered near-Earth space ($q < 1.3$ au), its instantaneous orbit every 10 kyr was recorded until it left near-Earth space or was removed from the simulation (either via collision with the Sun or a planet, or through ejection from the Solar system). These orbit

snapshots were compiled to build a probability map of where NEOs originating from this family would be found in orbital element space.

We show in Fig. 9 the preliminary probability maps from a test simulation. The highest probability spatial bins in each plot are shown in white (normalized probability of 1), with yellow, purple (50 per cent), blue and finally red showing decreasing probability density. Bins shown in black had a zero or near-zero recorded contribution from the simulated family members. Simulations of NEO evolution were conducted spanning a range of probable bulk densities (1500–2500 kg m^{-3}), but the simulated density had no significant effect on the resulting probability density map. The only difference of note is that due to the lower densities, the smallest objects in the simulation were more quickly moved into NEO space; thus, the overall flux of asteroids was a factor of $\simeq 4$ higher early in the simulations, decreasing to $\simeq 1.5$ times higher by the current age of the family as the slower, high-density test objects finally reach the resonances that push them into NEO space.

Future works will use a larger number of simulations to determine probability densities with higher accuracy, as individual runs can be dominated by a single long-lived object. In general, we find that NEAs from Rafita enter near-Earth space at similar semimajor axes and inclinations to the family ($a \sim 2.5$, $i \sim 8°$) as a result of eccentricity pumping. This phase space overlaps 8 per cent (1272 out of 15 091) of presently known NEAs. There is an immediate surge near $T = 0$ Myr in the NEA population from the small objects that are placed into the nearby resonances by the assumed impact generated velocities. After that, however, the family follows a steady injection rate for the rest of the simulation. Further follow-up would be, however, required to confirm a direct link between the NEOs and the Rafita family, since alternative pathways to produce these objects should also be studied. Quite interestingly, 4 per cent of the simulated objects that survived the last 30 Myr of the simulation seem to have rather different orbits from what the general heat map shows, with a cluster near 1 au. Confirming or denying the potential contribution of Rafita members to the observed population of potentially hazardous asteroids (PHA) remains an interesting challenge for future works.
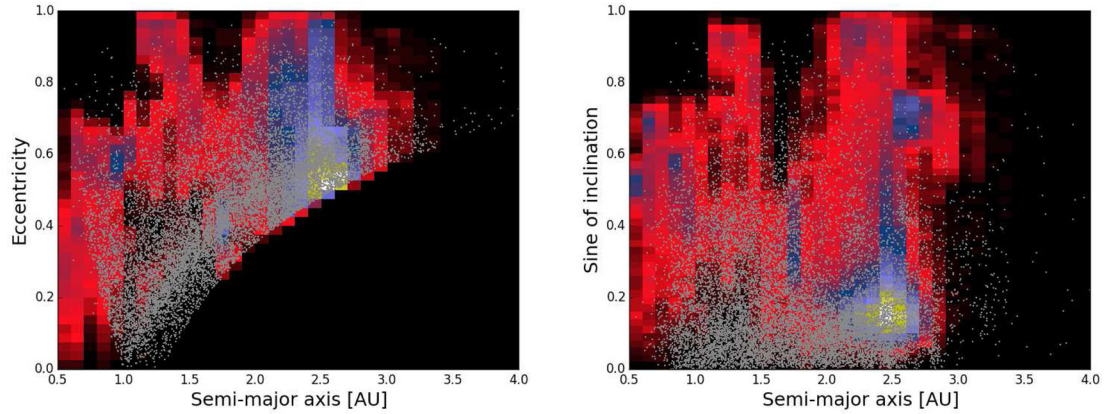
Figure 9. Probability map of NEAs originating from the Rafita family (background heat map) for semimajor axis versus eccentricity and semimajor axis versus the sine of inclination. Grey points indicate the orbits of all currently known NEAs.

7 CONCLUSION

Our results could be summarized as follows:

(i) We revised the current knowledge on the Rafita asteroid family. This group is an S-type family, with a few possible C-complex interlopers, and was most likely the product of a catastrophic disruption of a $D \simeq 45$ km parent body. The Rafita family is cut on the left-hand side in a by the 3J:-1A mean-motion resonance, and interacts with the $g + g_5 - 2g_6$ secular resonance.

(ii) We used the method of Yarkovsky isolines to eliminate possible dynamical interlopers, and Monte Carlo methods simulating the dynamical evolution of several fictitious asteroid families under the influence of the Yarkovsky and YORP effects. We find an age of 490^{+190}_{-220} Myr, and a value of the ejection velocity parameter $V_{\rm EJ}$ of 20^{+50}_{-20} m s^{-1}, comparable with the estimated escape velocity from the parent body ($\beta = \frac{V_{\rm EJ}}{V_{\rm esc}} = 0.71$).

(iii) We studied the dynamical evolution of fictitious members of the Rafita asteroid family simulating the initial conditions after breakup of the parent body and obtained new estimates of the family age using the method of the time dependence of the $\gamma_2(v_W)$ parameter (Carruba 2016) and a new method based on the time dependence of the coefficient A_S describing the asymmetry of the C distribution of the simulated Rafita family. Remarkably, these two methods provide estimates in good agreement with the results of the Yarko–YORP approach.

(iv) We studied the possible contribution to the NEA population from the Rafita family. One per cent of the simulated particles are NEOs in the last 10 Myr of the simulation, and $\simeq 40$ per cent of these cluster with semimajor axes near 1 au and could potentially contribute to the current population of PHA.

Overall, our results confirm and refine previous estimates of the Rafita family age, with a new estimate of 490 ± 200 Myr. More importantly, we introduced a new method to date the age of incomplete asteroid families based on the asymmetry coefficient of their C function distribution, which provided estimates of the family age in agreement with an independent method based on Monte Carlo simulations of the Yarkovsky and YORP dynamical evolution of family members and of the time evolution of the $\gamma_2(v_W)$ parameter. This new method can be potentially applied to other incomplete asteroid families, such as in the case of the Maria (interaction with the 3J:-1A mean-motion resonance) and Gefion (interaction with the 5J:-2A mean-motion resonance) families, and, in our opinion, represents the main result of this work.

REFERENCES

Bendjoya P., Zappalà V., 2002, in Bottke W. F., Jr, Cellino A., Paolicchi P., Binzel R. P., eds, Asteroids III. Univ. Arizona Press, Tucson, AZ, p. 613
Bottke W. F. et al., 2015, Icarus, 247, 191
Brož M., 1999, MsT. Charles Univ. Prague, Czech Republic
Brož M., Morbidelli A., Bottke W. F., Rozehnal J., Vokrouhlický D., Nesvorný D., 2013, A&A, 551, A117
Bus S. J., 1999, PhD thesis, Univ. Pittsburgh, p. 311
Bus S. J., Binzel R. P., 2002a, Icarus, 158, 106
Bus S. J., Binzel R. P., 2002b, Icarus, 158, 146
Carruba V., 2009, MNRAS, 395, 358
Carruba V., 2010, MNRAS, 408, 580
Carruba V., 2016, MNRAS, 461, 1605
Carruba V., Nesvorný D., 2016, MNRAS, 457, 1332
Carruba V., Burns J. A., Bottke W., Nesvorný D., 2003, Icarus, 162, 308
Carruba V., Roig F., Michtchenko T. A., Ferraz-Mello S., Nesvorný D., 2007, A&A, 465, 315
Carruba V., Aljbaae S., Souami D., 2014, ApJ, 792, 46
Carruba V., Nesvorný D., Aljbaae S., Huaman M. E., 2015, MNRAS, 451, 244
Carruba V., Nesvorný D., Marchi S., Aljbaae S., 2016, MNRAS, 458, 1117.
Delbo M., Mueller M., Emery J. P., Rozitis B., Capria M. T., 2015, in Michel P., DeMeo F. E., Bottke W., eds, Asteroid IV. Univ. Arizona Press, Tucson, AZ, p. 297
DeMeo F. E., Carry B., 2013, Icarus, 226, 723
Ivezić Ž. et al., 2001, AJ, 122, 2749
Kendall M.G., Stuart A., 1969, The Advanced Theory of Statistics, Volume 1: Distribution Theory, 3rd edn. Griffin, New York
Levison H. F., Duncan M. J., 1994, Icarus, 108, 18
Machuca J. F., Carruba V., 2012, MNRAS, 420, 1779

Masiero J. R. et al., 2011, ApJ, 741, 68

Masiero J. R., Mainzer A. K., Grav T., Bauer J. M., Jedicke R., 2012, ApJ, 759, 14

Masiero J., Carruba V., Mainzer A., Bauer J. M., Nugent C., 2015a, ApJ, 803, 179

Masiero J., DeMeo F., Kasuga T., Parker A. H., 2015b, in Michel P., DeMeo F. E., Bottke W., eds, Asteroid IV. Univ. Arizona Press, Tucson, AZ, p. 297

Morbidelli A., Vokrouhlický D., 2003, Icarus, 163, 120

Morbidelli A., Thomas F., Moons M., 1995, Icarus, 118, 322

Nesvorný D., Morbidelli A., 1998, AJ, 116, 3029

Nesvorny D., Broz M., Carruba V., 2015, in Michel P., DeMeo F. E., Bottke W., eds, Asteroid IV. Univ. Arizona Press, Tucson, AZ, p. 297

Press V. H., Teukolsky S. A., Vetterlink W. T., Flannery B. P., 2001, Numerical Recipes in Fortran 77. Cambridge Univ. Press, Cambridge

Spoto F., Milani A., Knežević Z., 2015, Icarus, 257, 275

Vokrouhlický D., Brož M., Morbidelli A., Bottke W. F., Nesvorný D., Lazzaro D., Rivkin A. S., 2006a, Icarus, 182, 92

Vokrouhlický D., Brož M., Bottke W. F., Nesvorný D., Morbidelli A., 2006b, Icarus, 182, 118

Vokrouhlický D., Brož M., Bottke W. F., Nesvorný D., Morbidelli A., 2006c, Icarus, 183, 349

Wisdom J., 1983, Icarus, 56, 51

This paper has been typeset from a TEX/LATEX file prepared by the author.